Theor Chem Acc (2010) 127:81–94
DOI 10.1007/s00214-009-0707-9

REGULAR ARTICLE

Theoretical study on the singlet and triplet potential energy surfaces of NH ($X^3\Sigma^-$) + HCNO reaction

Yang Gao · Xiu-Juan Jia · Sha Li · Yan-Bo Yu · Rong-Shun Wang · Xiu-Mei Pan

Received: 6 July 2009 / Accepted: 21 November 2009 / Published online: 6 January 2010

Abstract Both the singlet and triplet potential energy surfaces (PESs) of the NH ($X^3\Sigma^-$) + HCNO reaction have been investigated at the BMC-CCSD level based on the UB3LYP/6-311++G(d, p) structures. The results show that the title reaction is more favorable through the singlet potential energy surface than the triplet one. For the singlet potential energy surface of the NH ($X^3\Sigma^-$) + HCNO reaction, the most feasible association of NH ($X^3\Sigma^-$) with HCNO is found to be a non-barrier nitrogen-to-carbon attack forming the adduct **a** (*trans*-HNCHNO), which can isomerize to the adduct **b** (*cis*-HNCHNO). The most feasible channel is that the 1, 3-H shift with N2–H2 and C–N1 bonds cleavage associated with the N1–H2 bond formation of adduct **a** leads to the product $\mathbf{P_1}$ (HCN + HNO). Moreover, $\mathbf{P_2}$ (HNC + HNO) should be the competitive product. The other products, including $\mathbf{P_3}$ (NH_2 + NCO) and $\mathbf{P_4}$ (N_2H_2 + CO), are minor products. The product $\mathbf{P_1}$ can be obtained through two competitive channels Path 1: $\mathbf{R \rightarrow a \rightarrow P_1}$ and Path 3: $\mathbf{R \rightarrow b \rightarrow d \rightarrow P_1}$, whereas the product $\mathbf{P_2}$ can be formed through Path 2: $\mathbf{R \rightarrow b \rightarrow d \rightarrow P_2}$. At high temperatures, the nitrogen-to-nitrogen approach may become feasible. For the triplet potential energy surface of the NH ($X^3\Sigma^-$) + HCNO reaction, the Path 10: $\mathbf{R \rightarrow {}^3a \rightarrow {}^3a_1 \rightarrow P_1}$ should be the most feasible pathway due to the less reaction steps and lower barriers. These conclusions will have impacts on further experimental investigations.

Keywords NH ($X^3\Sigma^-$) · HCNO · Transition state · Mechanism · Potential energy surface

1 Introduction

Fulminic acid, HCNO, has recently been identified as an important intermediate in the NO-reburning process for the reduction of NO_x pollutants from fossil-fuel combustion emissions [1]. Thus, it is of great significance to learn the behavior of the HCNO radical for environmental protection. Hershberger and co-workers [2] studied the UV–Vis spectrum of HCNO, and believed that HCNO photolysis is probable. Several photolysis products are energetically possible at a 248 nm photolysis wavelength

$$\begin{aligned} \mathrm{HCNO} + h\nu\,(248\ \mathrm{nm}) &\rightarrow \mathrm{H} + \mathrm{NCO} \\ &\rightarrow \mathrm{HCN} + \mathrm{O} \\ &\rightarrow \mathrm{NH} + \mathrm{CO} \end{aligned}$$

Hershberger and co-workers speculated that these photolysis products of HCNO may have further reactions with HCNO. Up to now, the potential energy surfaces of the reactions between HCNO and NCO, H and O, which are all the photolysis products of HCNO, have been investigated both experimentally [2–4] and theoretically [5–9].

As the photolysis products of HCNO, the ground-state NH ($X^3\Sigma^-$) radical plays a significant role in many chemical processes, including combustion [10–12]. NH reactions are also important in reburning processes [13] and other techniques such as thermal de-NO_x reactions [14] for reduction of NO from combustion. This means the

Electronic supplementary material The online version of this article (doi:10.1007/s00214-009-0707-9) contains supplementary material, which is available to authorized users.

Y. Gao · X.-J. Jia · S. Li · Y.-B. Yu · R.-S. Wang · X.-M. Pan (✉)
Faculty of Chemistry, Institute of Functional Material Chemistry, Northeast Normal University, 130024 Changchun, People's Republic of China
e-mail: panxm460@nenu.edu.cn

reaction between the NH and HCNO may have a strong influence on models of both combustion and atmosphere chemistry.

In experiment, the NH + HCNO reaction has been studied by Hershberger and co-workers, all the products and the corresponding experimental values of ΔH°_{298} are shown as followed [2]:

$$\begin{aligned} \mathrm{NH} + \mathrm{HCNO} &\rightarrow \mathrm{CH_2O} + \mathrm{N_2}\ \Delta H^{\circ}_{298} = -158.8\ \mathrm{kcal/mol} \\ &\rightarrow \mathrm{NH_2} + \mathrm{NCO}\ \Delta H^{\circ}_{298} = -54.0\ \mathrm{kcal/mol} \\ &\rightarrow \mathrm{HCN} + \mathrm{HNO}\ \Delta H^{\circ}_{298} = -74.9\ \mathrm{kcal/mol} \end{aligned}$$

Recently, the triplet potential energy surface of the NH ($X^3\Sigma^-$) + HCNO reaction has been investigated by Chia-Chung Sun and co-workers [15]. This reaction also can occur in singlet. To our best knowledge, the singlet potential energy surface of the NH ($X^3\Sigma^-$) + HCNO reaction has not yet been reported. So, both the singlet and triplet potential energy surfaces of the NH ($X^3\Sigma^-$) + HCNO reaction have been studied in this work. What we have done is to complete the PES of the title reaction. All the possible reaction pathways are explored using DFT methods. The comparison between theoretical and experimental results on the predicted products and the values of ΔH°_{298} has been discussed. These investigations could provide useful information for further dynamical calculations and experimental studies.

2 Computational methods

All calculations are carried out using the Gaussian 03 program packages [16]. The geometries of all the reactants, products, intermediates, and transition states for the NH ($X^3\Sigma^-$) + HCNO reaction are optimized using hybrid density functional UB3LYP method (Becke's three parameter hybrid functional with the non-local correlation functional of Lee–Yang–Parr) [17, 18] with the 6-311++G(d, p) basis set. The stationary nature of structures is confirmed by harmonic vibrational frequency calculations, i.e., equilibrium species possess all real frequencies, whereas transition states possess one and only one imaginary frequency. The zero-point energy (ZPE) corrections are obtained at the same level of theory. To confirm that the transition state connects designated intermediates, intrinsic reaction coordinate (IRC) calculations [19, 20] are employed at the UB3LYP/6-311++G(d, p) level. In order to obtain more reliable energetic information, higher level single-point energy calculations are performed at the UQCISD(T)/6-311++G(d, p), UCCSD(T)/6-311++G(d, p) [21] and BMC-CCSD [22] levels using the UB3LYP/6-311++G(d, p) optimized geometries. Moreover, unless otherwise specified, the BMC-CCSD single-point energies with ZPE corrections are used in the following discussions.

3 Results and discussion

3.1 Singlet potential energy surface

The optimized structures of the reactants, products, intermediates and transition states as well as the available experimental [23, 24] and theoretical data [25] for the title reaction are depicted in Fig. 1. The harmonic vibrational frequencies including available experimental data [26, 27] are given in Table 1. The theoretical values are consistent with experimental ones. The relative energies including ZPE corrections of all species are summarized in Table 2. From Table 2 we can see that relative energies at QCISD(T)//B3LYP/6-311++G(d, p) and CCSD(T)//B3LYP/6-311++G(d, p) levels are close to each other, which are higher than that obtained from BMC-CCSD level. For our easier discussion, the energy of reactants **R** is set to be zero for reference. The symbol TSx/y is used to denote the transition state, where *x* and *y* are the corresponding intermediates or products. By means of the transition states and their connected isomers or products, a schematic potential energy surface of the NH ($X^3\Sigma^-$) + HCNO reaction in singlet is plotted in Fig. 2.

3.1.1 Initial association

On the singlet PES, the attack of N atom of NH ($X^3\Sigma^-$) radical on HCNO molecule may have two possible ways, i.e., nitrogen-to-carbon approach and nitrogen-to-nitrogen approach. The nitrogen-to-carbon approach is rather attractive to form adducts **a** (*trans*-HNCHNO) and **b** (*cis*-HNCHNO) without any encounter barrier. To further confirm the non-barrier of these processes, the point-wise potential energy curves at the B3LYP/6-311++G(d, p) level are calculated, and the results are shown in Figs. 1 and 2 of Supplementary Material, respectively. From Figs. 1 and 2, we know that adducts **a** and **b** are formed as the N atom of NH ($X^3\Sigma^-$) approaches the C atom of HCNO without barriers. The binding energies of **a** and **b** are −74.1 and −72.8 kcal/mol, respectively, which indicate that these processes make adducts **a** and **b** highly activated, and mean that further isomerization or dissociation reactions can be promoted. These associations are expected to be faster and will play a significant role in the reaction kinetics. Furthermore, adduct **a** can isomerize to **b** via the transition state **TSa/b**, as shown in Fig. 2. For the pathway of the N atom of NH ($X^3\Sigma^-$) radical attacking on the N atom of HCNO, the nitrogen-to-nitrogen approach can lead to adduct **c** (HCONNH)

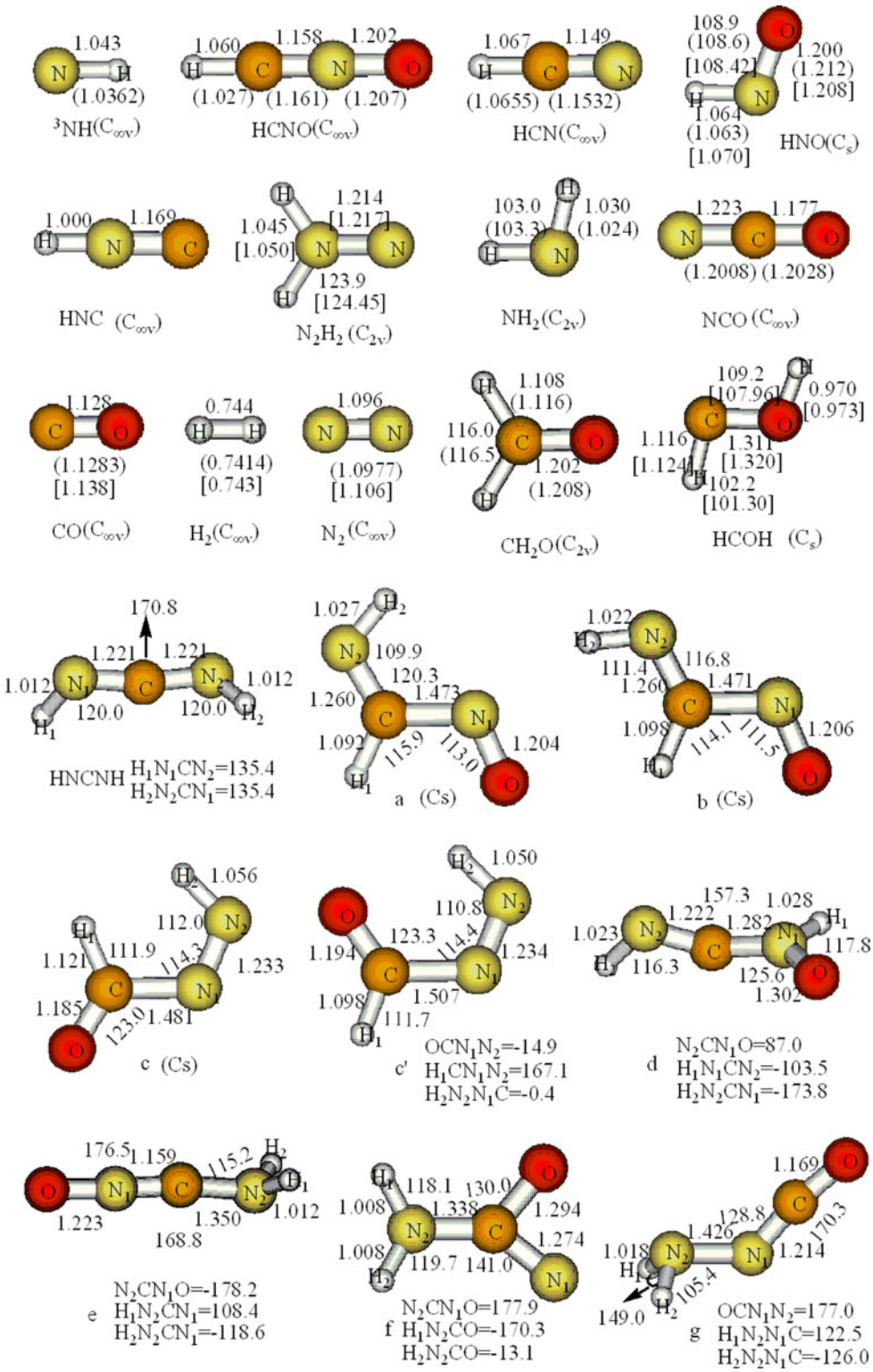

Fig. 1 B3LYP/6-311++G(d, p) optimized geometries of reactants, products, intermediates, and transition states. Bond distances are in angstroms and angles are in degrees. The values in "*brackets*" are the experimental values ([23] for NH, HCNO, HCN, HNO, NH_2, CO, H_2, N_2, CH_2CO; and [24] for NCO). The values in "*square brackets*" are the theoretical results, at the B3LYP/6-31G(d, p) level from [25]

with 95.9 kcal/mol below the reactants via a three-membered ring transition state **TSR/c** (0.7 kcal/mol). It is obviously, the adduct **c** is an energy rich intermediate, and this indicates that further isomerization or dissociation reactions can be promoted. Therefore, in the following discussions, we mainly discuss the formation pathways of various products starting from adducts **a**, **b**, or **c**.

Fig. 1 continued

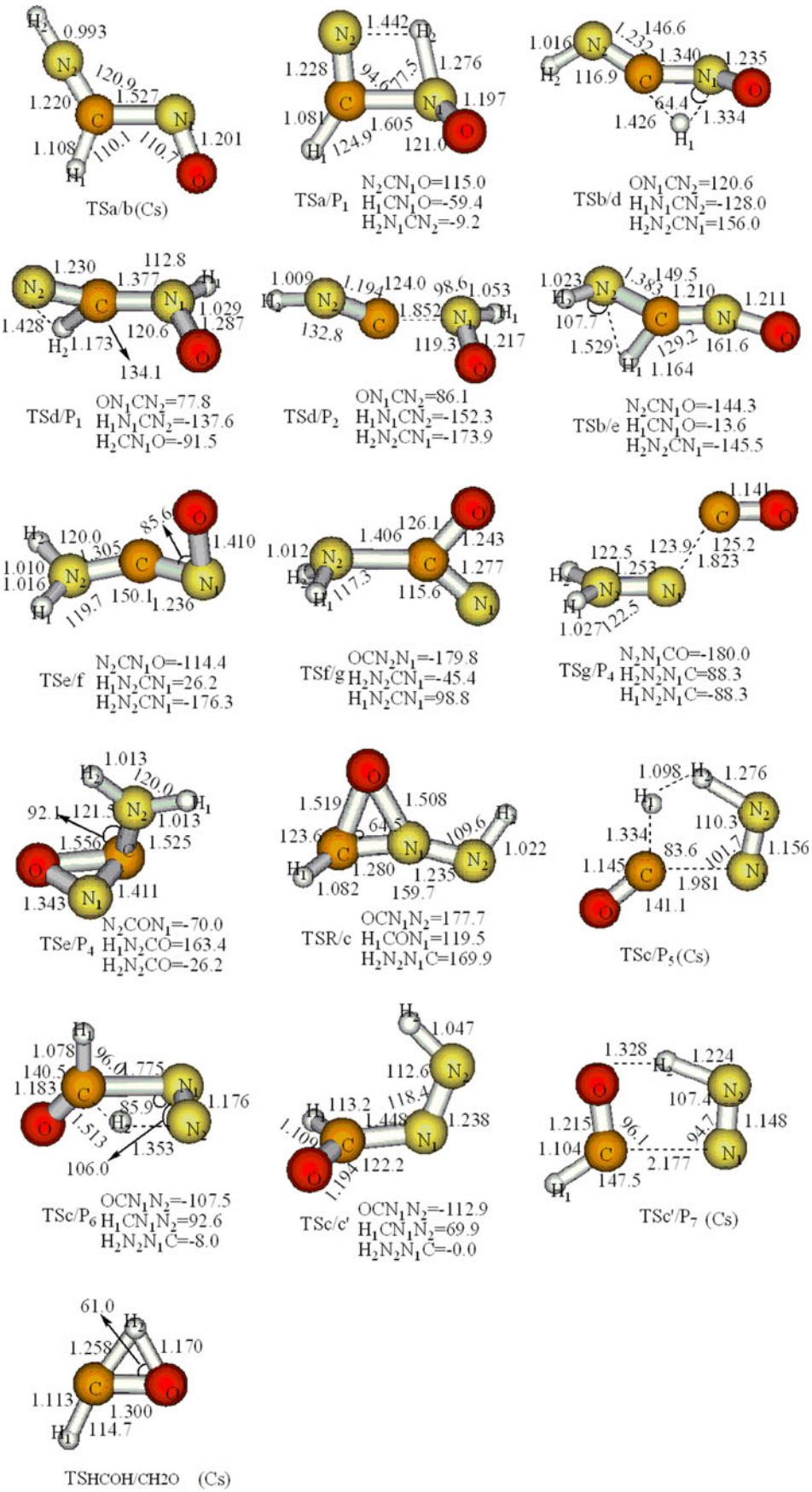

Table 1 Calculated and experimental frequencies (cm^{-1}) of the reactants, products, intermediates and transition states for the NH ($X^3\Sigma^-$) + HCNO reaction in singlet at the B3LYP/6-311++G(d, p) level

Species	Frequencies
NH	3,254 (3,282)[a]
HCNO	271, 367, 558, 1,287, 2,321, 3,508
HCN	768, 768, 2,195, 3,449
HNC	495, 495, 2,095, 3,807
HNO	1,564, 1,671, 2,864 (1,511, 1,569, 2,854)[b]
NCO	502, 585, 1,297, 1,995
NH_2	1,507, 3,352, 3,443
N_2H_2	1,025, 1,335, 1,612, 1,747, 3,000, 3,034
CO	2,212
CH_2O	1,202, 1,260, 1,531, 1,815, 2,884, 2,942
HCOH	1,100, 1,218, 1,323, 1,505, 2,851, 3,711
H_2	4,419
N_2	2,445
a	134, 374, 580, 801, 946, 1,112, 1,216, 1,352, 1,630, 1,713, 3,108, 3,407
b	140, 408, 600, 772, 918, 1,110, 1,205, 1,360, 1,624, 1,712, 3,033, 3,469
c	120, 433, 603, 851, 961, 1,079, 1,361, 1,483, 1,637, 1,873, 2,792, 2,964
c′	69, 376, 707, 791, 902, 1,105, 1,351, 1,484, 1,637, 1,817, 3,042, 3,075
d	226, 265, 643, 689, 840, 998, 1,108, 1,213, 1,490, 2,086, 3,327, 3,436
e	76, 222, 372, 499, 584, 890, 1,191, 1,411, 1,646, 2,479, 3,522, 3,608
f	275, 411, 439, 462, 618, 1,018, 1,046, 1,403, 1,614, 1,833, 3,592, 3,711
g	33, 207, 593, 653, 864, 1,066, 1,330, 1,451, 1,678, 2,312, 3,463, 3,532
TSa/b	1031*i*, 109, 394, 524, 704, 890, 916, 1,323, 1,643, 1,829, 2,920, 3,894
TSa/P_1	1570*i*, 302, 313, 654, 801, 858, 1,059, 1,261, 1,574, 1,776, 1,945, 3,235
TSb/d	1491*i*, 256, 391, 669, 726, 840, 968, 1,077, 1,426, 1,797, 1,853, 3,550
TSd/P_1	1416*i*, 199, 324, 484, 606, 653, 979, 1,206, 1,484, 1,861, 2,649, 3,314
TSd/P_2	431*i*, 111, 351, 419, 553, 609, 930, 1,489, 1,529, 1,938, 2,995, 3,666
TSb/e	1255*i*, 233, 250, 448, 528, 828, 910, 1,172, 1,387, 2,082, 2,593, 3,441
TSe/P_4	423*i*, 393, 504, 572, 761, 786, 948, 1,037, 1,267, 1,551, 3,495, 3,655
TSe/f	558*i*, 189, 306, 464, 545, 853, 1,116, 1,169, 1,641, 1,975, 3,491, 3,624
TSf/g	391*i*, 270, 422, 486, 620, 960, 1,099, 1,475, 1,563, 1,621, 3,544, 3,662
TSg/P_4	442*i*, 100, 285, 436, 559, 808, 1,285, 1,438, 1,711, 2,080, 3,276, 3,338
TSR/c	394*i*, 400, 458, 592, 731, 905, 1,048, 1,183, 1,277, 1,898, 3,204, 3,464
TSc/P_5	1442*i*, 42, 203, 584, 740, 768, 1,212, 1,373, 1,421, 1,656, 2,002, 2,099
TSc/P_6	1605*i*, 334, 394, 584, 697, 942, 1,039, 1,164, 1,528, 1,806, 1,886, 3,267
TSc/c′	179*i*, 302, 499, 792, 1,028, 1,059, 1,369, 1,473, 1,647, 1,826, 2,916, 3,066
TSc′/P_7	948*i*, 354, 431, 673, 698, 736, 1,201, 1,269, 1,718, 1,752, 2,051, 2,963
TSHCOH/CH_2O	2111*i*, 743, 1,317, 1,428, 2,608, 2,879

[a] Experimental values from [26]

[b] Experimental values from [27]

3.1.2 *Isomerization and dissociation pathways*

3.1.2.1 The nitrogen-to-carbon approach *Starting from adduct* ***a*** The initial adduct **a** (*trans*-HNCHNO) is a stable and branched chainlike isomer with C_1 symmetry. From the PES (Fig. 2), **a** can easily lead to product $\mathbf{P_1}$ (HCN + HNO) which had been observed by Hershberger in experiment [2] via a non-planar transition state $\mathbf{TSa/P_1}$ (−33.4 kcal/mol). As seen in Fig. 1, the C_1 symmetried $\mathbf{TSa/P_1}$ has a loose CN1H2N2 four-membered ring structure, in which the forming H2–N1 bond length is 1.276 Å, while the breaking N2–H2 and C–N1 bonds length are 1.442 and 1.605 Å, respectively. The vibration mode of the imaginary frequency of $\mathbf{TSa/P_1}$ with 1570*i* cm^{-1} corresponds to H2–N1, N2–H2 and C–N1 bonds stretch vibrations. This pathway can be expected as the dominant channel. Such a process can be described as

$$\text{Path 1}: \mathbf{R} \rightarrow \mathbf{a} \rightarrow \mathbf{P_1}\,(\text{HCN} + \text{HNO})$$

Starting from adduct ***b*** The adduct **b** (*cis*-HNCHNO) is another nitrogen-to-carbon approaching isomer. Its branched chainlike structure is similar to adduct **a** (*trans*-HNCHNO),

Table 2 Zero-point energies (ZPE) (a.u.) and relative energies E_{rel} (kcal/mol) (with inclusion of the B3LYP/6-311++G(d, p) ZPE corrections) of the reactants, products, intermediates and transition states for the NH ($X^3\Sigma^-$) + HCNO reaction in singlet at different levels

Species	ZPE B3LYP/ 6-311++G(d, p)	E_{rel} QCISD(T)//B3LYP/ 6-311++G(d, p) + ZPE	E_{rel} CCSD(T)//B3LYP/ 6-311++G(d, p) + ZPE	E_{rel} BMC-CCSD//B3LYP/ 6-311++G(d, p) + ZPE
R: NH($X^3\Sigma^-$) + HCNO	0.026349	0.0	0.0	0.0
P_1: HCN + HNO	0.030254	−67.9	−68.3	−68.5
P_2: HNC + HNO	0.029597	−53.3	−53.6	−53.8
P_3: NH2 + NCO	0.027480	−51.7	−51.6	−50.8
P_4: N2H2 + CO	0.031823	−80.9	−81.1	−79.2
P_5: H2 + N2 + CO	0.020677	−157.2	−157.4	−153.1
P_6: CH2O + N2	0.032075	−151.2	−150.9	−150.7
P_7: HCOH + N2	0.032242	−99.8	−100.2	−98.9
a	0.037299	−72.3	−72.7	−74.1
b	0.037234	−71.0	−71.4	−72.8
c	0.036811	−93.3	−93.6	−95.9
c′	0.037263	−94.3	−94.6	−97.0
d	0.037180	−47.0	−46.9	−53.9
e	0.037540	−65.3	−65.0	−74.6
f	0.037411	−71.3	−71.2	−76.6
g	0.039140	−108.1	−108.2	−113.8
TSa/b	0.034507	−46.8	−47.2	−50.2
TSa/P_1	0.031390	−32.6	−32.3	−33.4
TSb/d	0.030879	−15.4	−14.9	−19.9
TSd/P_1	0.031344	−0.7	−5.0	−5.5
TSd/P_2	0.033242	−32.2	−32.1	−33.7
TSb/e	0.031601	−0.9	−0.02	−6.8
TSe/P_4	0.034102	6.9	7.1	3.1
TSe/f	0.035023	−31.8	−31.3	−37.2
TSf/g	0.035814	−61.9	−59.7	−61.4
TSg/P_4	0.034890	−64.9	−65.0	−65.5
TSR/c	0.034542	5.0	4.9	0.7
TSc/P_5	0.027562	−77.3	−77.4	−78.1
TSc/P_6	0.031078	−50.5	−50.4	−52.2
TSc/c′	0.036398	−90.9	−91.2	−93.5
TSc′/P_7	0.031546	−71.3	−71.5	−72.9
TSP_7/P_6	0.026014	−68.3	−68.4	−68.3

and it only lies 1.3 kcal/mol higher than **a**. They can isomerize to each other via **TSa/b** (−50.2 kcal/mol). Moreover, the adduct **b** can isomerize to a non-planar isomer **d** (HNCNHO) via **TSb/d** (−19.9 kcal/mol), which is a 1, 2-H shift process. The vibration mode of imaginary frequency 1,491*i* cm^{-1} corresponds to C–H1 and H1–N1 bonds stretch vibrations. The migrating hydrogen is 1.426 Å away from the origin (C atom) and 1.334 Å away from the migrating terminus (N1 atom). Subsequently, isomer **d** can take a C–N1 bond rupture via transition state **TSd/P$_2$** with the barrier of 20.2 kcal/mol leading to product **P$_2$** (HNC + HNO). The weak-bond structure of **TSd/P$_2$** is characterized by a markedly elongated C–N1 bond (1.852 Å). Alternatively, the isomer **d** may proceed to product **P$_1$** (HCN + HNO) via a loose CN2H2 three-membered ring transition state **TSd/P$_1$** with the barrier of 48.4 kcal/mol. Apparently, this channel is not as competitive as Path 1. Note that the isomerization between HCN and HNC has been the focus of many studies [28, 29], so we do not describe it in this work. These processes can simply be written as

Path 2 : **R** → **b** → **d** → **P$_2$**(HNC + HNO)

Path 3 : **R** → **b** → **d** → **P$_1$**(HCN + HNO)

In addition, the adduct **b** can isomerize to a non-planar isomer **e** (HHNCNO) of C_{2v} symmetry structure via 1, 2-H

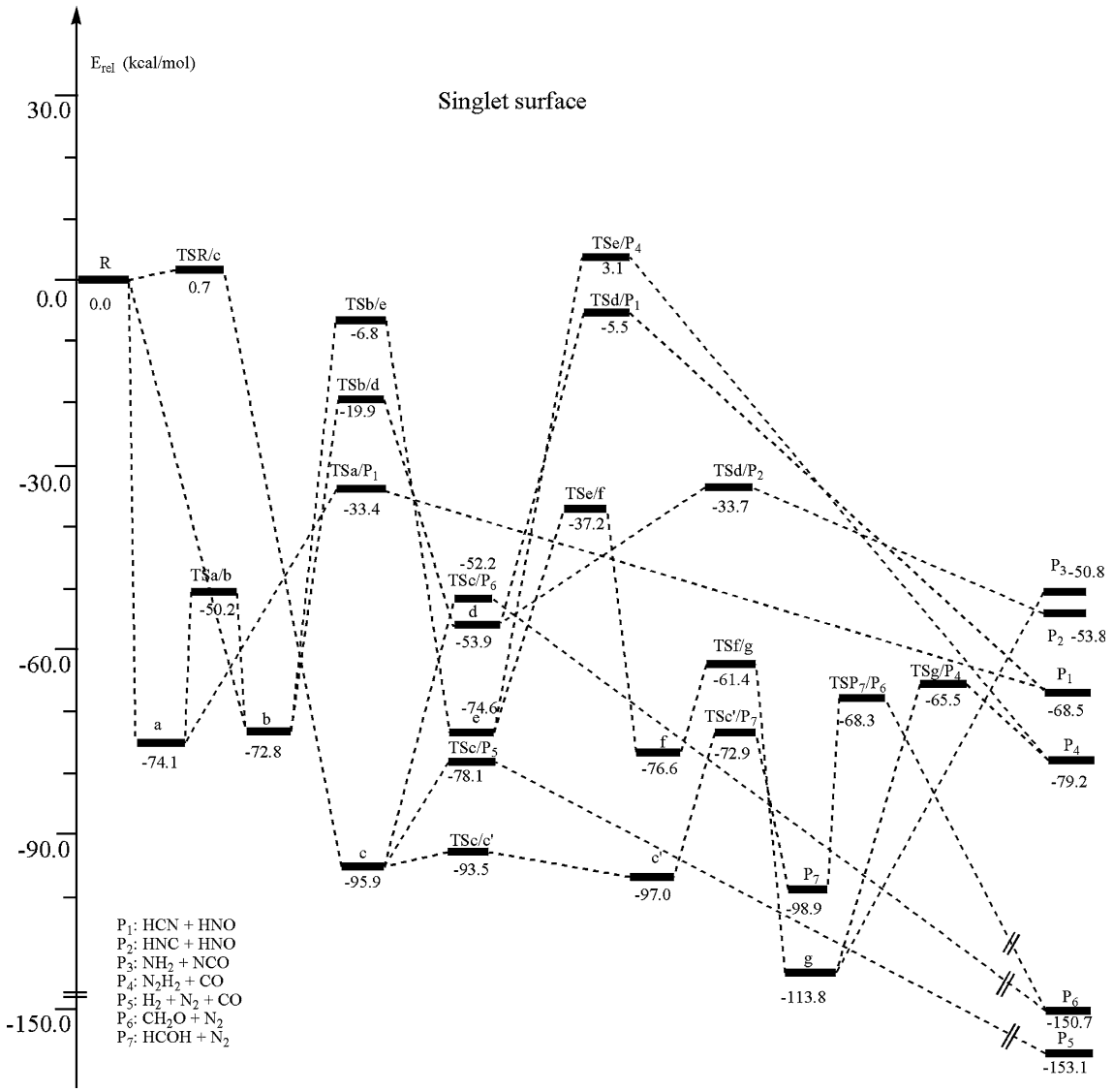

Fig. 2 Schematic potential energy surface of the reaction channels for the NH ($X^3\Sigma^-$) + HCNO reaction in singlet. Relative energies (E_{rel}, kcal/mol) are calculated at the BMC-CCSD//B3LYP/6-311++G(d, p) level

shift from C to N2 atom (i.e., **TSb/e**) with a barrier of 66.0 kcal/mol. The migrating hydrogen atom is 1.164 Å away from the origin (C atom) and 1.529 Å away from the migrating terminus (N2 atom). Subsequently, the isomer **e** can rearrangement to **g** (HHNNCO) via **TSe/f** and **TSf/g**, which lie below the reactants by 37.2 and 61.4 kcal/mol, respectively. The loose CN1O three-membered ring structure is found in **TSe/f**. The vibration mode of imaginary frequency 558*i* cm^{-1} corresponds to C–O and N1–O bonds stretch vibrations. The migrating oxygen in **TSe/f** is 1.410 Å away from the origin (N1 atom) and 1.803 Å away from the migrating terminus (C atom). And isomer **f** can undergo C–N2 bond cleavage along with N1–N2 bond formation to form **g** via **TSf/g**. The isomer **g** can either directly dissociate to product $\mathbf{P_3}$ (NH_2 + NCO) which had been observed by Hershberger in experiment [2] through the long N1–N2 weak-bond (1.426 Å) cleavage or taking a C–N2 bond rupture via transition state $\mathbf{TSg/P_4}$ with the barrier of 48.3 kcal/mol leading to product $\mathbf{P_4}$ (N_2H_2 + CO). The relative energy of $\mathbf{P_4}$ is −79.2 kcal/mol, that is lower than $\mathbf{P_3}$ (−50.8 kcal/mol) by 28.4 kcal/mol. Therefore, it can be predicted that $\mathbf{P_4}$ would be obtained. The transition state $\mathbf{TSg/P_4}$ is characterized by a markedly enlongated C–N2 bond (1.824 Å) and a compressed N1–N2 bond (1.253 Å). Furthermore, $\mathbf{P_4}$ (N_2H_2 + CO) is also produced by another pathway, it can be obtained through a loose three-membered ring transition state $\mathbf{TSe/P_4}$ (3.1 kcal/mol) from isomer **e**. The

high energy (3.1 kcal/mol above the reactants) makes this channel not competitive for $\mathbf{P_4}$ formation. These processes can be described as

Path 4 : $\mathbf{R} \rightarrow \mathbf{b} \rightarrow \mathbf{e} \rightarrow \mathbf{f} \rightarrow \mathbf{g} \rightarrow \mathbf{P_3}(NH_2 + NCO)$

Path 5 : $\mathbf{R} \rightarrow \mathbf{b} \rightarrow \mathbf{e} \rightarrow \mathbf{f} \rightarrow \mathbf{g} \rightarrow \mathbf{P_4}(N_2H_2 + CO)$

Path 6 : $\mathbf{R} \rightarrow \mathbf{b} \rightarrow \mathbf{e} \rightarrow \mathbf{P_4}(N_2H_2 + CO)$

3.1.2.2 The nitrogen-to-nitrogen approach The adduct **c** (HCONNH) is formed via **TSR/c** with the barrier of 0.7 kcal/mol. The non-planar **TSR/c** has a tight CN1O three-membered ring structure, in which the forming C–O bond length is 1.519 Å. It should be pointed out that the high-energy transition state **TSR/c,** which lies above the reactants, causes that the process from R → c is kinetically less feasible at normal temperatures. However, since the R → c conversion barrier is just 0.7 kcal/mol above the reactants, the conversion may become feasible at high temperatures. Isomer **c** then can easily lead to product $\mathbf{P_5}$ ($H_2 + N_2 + CO$) via $\mathbf{TSc/P_5}$ (−78.1 kcal/mol). The planar CN1N2H2H1 five-membered ring structure is found in $\mathbf{TSc/P_5}$. The vibration mode of imaginary frequency 1,442*i* cm^{-1} corresponds to C–H1, H1–H2 and N2–H2 bonds stretch vibrations. In addition, the planar isomer **c** also can undergo a loose CN1N2H2 four-membered ring transition state $\mathbf{TSc/P_6}$ (−52.2 kcal/mol) to give product $\mathbf{P_6}$ ($CH_2O + N_2$) which had been observed by Hershberger in experiment [2]. The corresponding forming C–H2 bond length is 1.531 Å, while the breaking C–N1 and H2–N2 bonds distances are 1.775 and 1.353 Å, respectively. The imaginary frequency of 1,650*i* cm^{-1} mainly involves the stretch vibrations of C–H2, C–N1 and H2–N2 bonds. Alternatively, the planar isomer **c** can take a C–N1 bond rotation process to form a non-planar isomer **c′** via **TSc/c′** with the barrier of 2.4 kcal/mol. Subsequently, isomer **c′** can take a 1, 4-H shift with C–N1 and N2–H2 bonds rupture along with O–H2 bond formation leading to product $\mathbf{P_7}$ ($HCOH + N_2$) via $\mathbf{TSc'/P_7}$ (−72.9 kcal/mol). The loose CN1N2H2O five-membered ring, which is planar, is found in $\mathbf{TSc'/P_7}$. The migrating hydrogen is 1.224 Å from the origin (N2 atom) and 1.328 Å away from the migrating terminus (O atom), and the breaking C–N1 bond is surprisingly long as 2.117 Å. In addition, the product HCOH of $\mathbf{P_7}$ can isomerize to CH_2O of $\mathbf{P_6}$ via 1, 2-H shift from O to C atom (i.e., **TSHCOH/CH_2O**), the N_2 molecule keeps unchanged in the subprocess $\mathbf{P_7} \rightarrow \mathbf{P_6}$ [30]. Via the transition state **TSHCOH/CH_2O**, the hydrogen atom in HCOH migrates from the place, where the O–H bond is cleaved, to link with the intramolecular C to produce CH_2O. These processes can be written as

Path 7 : $\mathbf{R} \rightarrow \mathbf{c} \rightarrow \mathbf{P_5}(H_2 + N_2 + CO)$

Path 8 : $\mathbf{R} \rightarrow \mathbf{c} \rightarrow \mathbf{P_6}(CH_2O + N_2)$

Path 9 : $\mathbf{R} \rightarrow \mathbf{c} \rightarrow \mathbf{c'} \rightarrow \mathbf{P_7}(HCOH + N_2) \rightarrow \mathbf{P_6}(CH_2O + N_2)$

3.1.3 Reaction mechanism and experimental implications

As present in the proceeding sections, we have obtained nine reaction channels (Paths 1–9) for the singlet PES of the NH ($X^3\Sigma^-$) + HCNO reaction. The nitrogen-to-carbon approach forms the low-lying adducts **a** (*trans*-HNCHNO) and **b** (*cis*-HNCHNO). Starting from **a**, there is only one channel (Path 1) leading to product $\mathbf{P_1}$ (HCN + HNO) via $\mathbf{TSa/P_1}$ (−33.4 kcal/mol). Furthermore, isomer **a** most favorably isomerizes to **b**. The adduct **b** can isomerize to either **d** via **TSb/d** (−19.9 kcal/mol) or **e** via **TSb/e** (−6.8 kcal/mol). Obviously, Paths 2 and 3 which are related to isomer **d** leading to $\mathbf{P_2}$ (HNC + HNO) and $\mathbf{P_1}$ (HCN + HNO), respectively, are more feasible than Paths 4–6 which are related to isomer **e** leading to $\mathbf{P_3}$ ($NH_2 + NCO$) and $\mathbf{P_4}$ ($N_2H_2 + CO$). With respect to these pathways, Paths 1–3 should be more competitive than the other channels due to the less reaction steps and lower barriers. Paths 4–6 are the less competitive channels. Paths 7–9, which are nitrogen-to-nitrogen approach channels, leading to products $\mathbf{P_5}$ ($H_2 + N_2 + CO$), $\mathbf{P_6}$ ($CH_2O + N_2$) and $\mathbf{P_7}$ ($HCOH + N_2$) are the less competitive pathways at normal temperatures, because of the higher energy of **TSR/c** which lies above the reactants by 0.7 kcal/mol, and may be of significance only at high temperatures. As a result, reflected in the final distributions, we predict that (1) $\mathbf{P_1}$ is the most favorable product; (2) $\mathbf{P_2}$ is the second favorable product; (3) $\mathbf{P_3}$ and $\mathbf{P_4}$ are the less competitive products; (4) the formation of products $\mathbf{P_5}$, $\mathbf{P_6}$, and $\mathbf{P_7}$ may become possible only at high temperatures. Furthermore, the product $\mathbf{P_7}$ ($HCOH + N_2$) can isomerize to the product $\mathbf{P_6}$ ($CH_2O + N_2$).

In Hershberger's study, they observed the products $\mathbf{P_1}$ (HCN + HNO), $\mathbf{P_3}$ ($NH_2 + NCO$), and $\mathbf{P_6}$ ($CH_2O + N_2$) in experiment, and the corresponding experimental values of $\Delta H°_{298}$ are −74.9, −54.0, and −158.8 kcal/mol, respectively [2]. In our theoretical investigations, $\mathbf{P_1}$, $\mathbf{P_3}$, and $\mathbf{P_6}$ have been obtained, the corresponding theoretical and experimental values of $\Delta H°_{298}$ are shown in Table 3. The theoretical values of $\Delta H°_{298}$ are calculated at the higher levels of G3MP2, BMC-CCSD, CCSD(T)/cc-pVTZ, QCISD(T) and CCSD(T) with 6-311++G(d, p) basis set. From Table 3, we can see that the theoretical values of $\Delta H°_{298}$ at QCISD(T) and CCSD(T) levels are consistent with each other. However, the BMC-CCSD level is more

Table 3 Theoretical values of $\Delta H°_{298}$ (kcal/mol) of reactants and products calculated at QCISD(T)/6-311++G(d, p), CCSD(T)/6-311++G(d, p), G3MP2, CCSD(T)/cc-pVTZ and BMC-CCSD levels

Reactants and products	QCISD(T)/ 6-311++G(d, p)	CCSD(T)/ 6-311++G(d, p)	G3MP2	CCSD(T)/cc-pVTZ	BMC-CCSD	Experiment[a]
R: NH ($X^3\Sigma^-$) + HCNO	0.0	0.0	0.0	0.0	0.0	0.0
P_1: HCN + HNO	−68.5	−68.8	−67.4	−67.9	−71.5	−74.9
P_2: HNC + HNO	−53.6	−54.0				
P_3: NH_2 + NCO	−51.9	−51.8	−54.0	−50.7	−51.0	−54.0
P_4: N_2H_2 + CO	−81.5	−81.7				
P_5: H_2 + N_2 + CO	−156.1	−156.2				
P_6: CH_2O + N_2	−151.8	−152.1	−149.9	−151.2	−154.9	−158.8
P_7: HCOH + N_2	−100.4	−100.7				

[a] Experimental values from [2]

reliable because the values of $\Delta H°_{298}$ in this level are close to the corresponding experimental value.

As shown in Table 2, the relative energies of these species are calculated at QCISD(T)//B3LYP/6-311++G(d, p), CCSD(T)//B3LYP/6-311++G(d, p) and BMC-CCSD//B3LYP/6-311++G(d, p) levels. On the basis of our present calculations, we expect that **P_5** (H_2 + N_2 + CO) is more competitive than **P_6** (CH_2O + N_2), because the transition state **TSc/P_5** in Path 7 lies 25.9 kcal/mol lower than **TSc/P_6** in Path 8. Because **P_6** has been observed in the experiment, we consider that **P_5** should be observed. For the existence of the isomerization between HCN and HNC [28, 29], it is expected that **P_2** (HNC + HNO), which is obtained in the theoretical calculations, can also be observed in experiment. Therefore, our theoretical result presented here is expected to provide useful information for the further investigation.

3.2 Triplet potential energy surface

The triplet reaction mechanism and the potential energy surface of the title reaction have been studied by Chia-Chung Sun and co-workers [15]. The multiple-channel reactions are investigated in detail, including the direct H-abstraction and a series of addition–elimination mechanism. The main product in their study is **^{1}HCN** + **^{3}HON**, and the reaction processes by H-shift and C–N bond cleavage from a favorable intermediate **HNCHNO**. In order to complete the triplet potential energy surface, in the following discussions, we are concerned about the formation channels of the other products as a supplementary study, which are different from that of Chia-Chung Sun and co-workers' studies but predict in experiment [2].

In our studies, the N–C attacking can form the common favorable intermediate **HNCHNO**, which is same to Sun's studies. We exhibit two isomeric forms of **HNCHNO**, **^{3}a** (*trans*-HNCHNO) and **^{3}b** (*cis*-HNCHNO) lying below the reactants by 59.0 and 58.1 kcal/mol, respectively, they are all approximately 15 kcal/mol higher than that of the singlet species **a** and **b**. Therefore, **^{3}a** and **^{3}b** are thermodynamically less favorable than **a** and **b**. And they can isomerize to each other via **TS^{3}a/^{3}b** (−36.2 kcal/mol). As seen in Figs. 3 and 4 of Supplementary Material, respectively, the point-wise potential energy curves of **^{3}a** and **^{3}b** at the UB3LYP/6-311++G(d, p) level show that they are formed without barriers. The nitrogen-to-nitrogen attacking can form isomer **^{3}c** (*cis*-OCHNNH) via **TSR/^{3}c** with the barrier of 51.9 kcal/mol, which is much higher than singlet **TSR/c** (0.7 kcal/mol). Therefore, formation of **^{3}c** is thermodynamically almost prohibited. Note that the optimized structures and corresponding energies of the relevant isomers and transition states in triplet are included in Fig. 3 and Table 4. The triplet PES of the NH + HCNO reaction is shown in Fig. 4.

3.2.1 The nitrogen-to-carbon approach

3.2.1.1 Starting from adduct ^{3}a The adduct **^{3}a** (*trans*-HNCHNO) isomerizes to **^{3}a$_1$** (HNCNHO) via 1, 3-H shift transition state **TS^{3}a/^{3}a$_1$** (−3.7 kcal/mol), The planar **TS^{3}a/^{3}a$_1$** has a loose H2N2CN1 four-membered ring structure, in which the forming N1–H2 bond length is 1.331 Å while the breaking N2–H2 bond length is 1.429 Å. The planar isomer **^{3}a$_1$** dissociates to **P_1** (HCN + HNO) via **TS^{3}a$_1$/P_1** (−30.6 kcal/mol), and the breaking C–N1 bond is 1.871 Å. Kinetically, this channel is competitive due to the less reaction steps and lower energy barriers. Alternatively, the adduct **^{3}a** can isomerize to **^{3}a$_2$** (HHNCNO) via 1, 2-H shift (**TS^{3}a/^{3}a$_2$**), followed by rearrangement to **^{3}a$_4$** (HHNCNO) via 1, 2-O shift (**TS^{3}a$_2$/^{3}a$_3$**, **TS^{3}a$_3$/^{3}a$_4$**). Then **^{3}a$_4$** can take a N1–C bond rupture via transition state **TS^{3}a$_4$/P_3** (−40.8 kcal/mol) leading to product **P_3** (NH_2 + NCO). The barrier height

Table 4 Zero-point energies (ZPE) (a.u.) and relative energies E_{rel} (kcal/mol) (with inclusion of the UB3LYP/6-311++G(d, p) ZPE corrections) of the reactants, products, intermediates and transition states for the NH ($X^3\Sigma^-$) + HCNO reaction in triplet at different levels

Species	ZPE UB3LYP/ 6-311++G(d, p)	E_{rel} UQCISD(T)//UB3LYP/ 6-311++G(d, p) + ZPE	E_{rel} UCCSD(T)//UB3LYP/ 6-311++G(d, p) + ZPE	E_{rel} BMC-CCSD//UB3LYP/ 6-311++G(d, p) + ZPE
R: NH($X^3\Sigma^-$) + HCNO	0.026349	0.0	0.0	0.0
P_1: HCN + HNO	0.030254	−67.9	−68.3	−68.5
P_2: HNC + HNO	0.029597	−53.3	−53.6	−53.8
P_3: NH_2 + NCO	0.027480	−51.7	−51.6	−50.8
P_4: N_2H_2 + CO	0.031823	−80.9	−81.1	−79.2
P_8: O + HNCNH	0.032585	−31.5	−31.9	−28.7
^3a	0.036850	−56.8	−56.8	−59.0
$^3a_1$	0.036190	−43.6	−43.8	−44.2
$^3a_2$	0.037169	−38.5	−38.5	−40.6
$^3a_3$	0.036355	−18.7	−18.9	−20.2
$^3a_4$	0.036742	−80.1	−80.2	−80.2
^3b	0.036975	−56.0	−56.1	−58.1
$^3b'$	0.037406	−55.8	−55.9	−58.2
$^3b_1$	0.036971	−35.0	−35.2	−37.3
^3c	0.035962	−60.1	−60.1	−62.2
$^3c'$	0.034992	−59.8	−59.9	−62.3
$^3c_1$	0.036787	−63.7	−63.8	−65.7
$TS^3a/^3b$	0.033752	−33.5	−33.4	−36.2
$TS^3a/^3a_1$	0.031231	−2.6	−1.6	−3.7
TS^3a_1/P_1	0.031765	−29.7	−29.5	−30.6
$TS^3a/^3a_2$	0.030084	11.7	11.9	9.8
$TS^3a_2/^3a_3$	0.035596	−5.6	−5.3	−6.7
$TS^3a_3/^3a_4$	0.034654	6.7	−3.8	−4.6
TS^3a_4/P_3	0.031645	−42.6	−42.3	−40.8
$TS^3b/^3b'$	0.036332	−48.0	−48.3	−48.7
$TS^3b'/^3b_1$	0.029967	15.3	15.7	12.9
TS^3b_1/P_2	0.031068	−17.6	−17.6	−18.1
TS^3b_1/P_8	0.033499	−9.6	−9.3	−9.8
$TSR/^3c$	0.032849	53.8	53.6	51.9
$TS^3c/^3c'$	0.034476	−54.4	−54.5	−55.7
$TS^3c'/^3c_1$	0.029521	−21.6	−21.3	−25.1
TS^3c_1/P_3	0.032209	−29.4	−28.8	−31.3
TS^3c_1/P_4	0.033795	−55.5	−55.7	−53.0

of $\mathbf{TS^3a/^3a_2}$, $\mathbf{TS^3a_2/^3a_3}$ and $\mathbf{TS^3a_3/^3a_4}$ are 9.8, −6.7 and 4.6 kcal/mol, respectively. Apparently, this channel is not competitive for the $\mathbf{P_3}$ formation. These processes can be described as

$$\text{Path 10}: \mathbf{R} \rightarrow {}^3\mathbf{a} \rightarrow {}^3\mathbf{a}_1 \rightarrow \mathbf{P_1}\,(\text{HCN} + \text{HNO})$$

$$\text{Path 11}: \mathbf{R} \rightarrow {}^3\mathbf{a} \rightarrow {}^3\mathbf{a}_2 \rightarrow {}^3\mathbf{a}_3 \rightarrow {}^3\mathbf{a}_4 \rightarrow \mathbf{P_3}\,(\text{NH}_2 + \text{NCO})$$

3.2.1.2 Starting from adduct $^3\boldsymbol{b}$ The planar isomer $^3\mathbf{b}$ (*cis*-HNCHNO) can take a C–N1 bond rotation process to form a planar isomer $^3\mathbf{b}'$ (*trans*-HNCHNO) via $\mathbf{TS^3b/^3b'}$ with the barrier of 9.4 kcal/mol, then $^3\mathbf{b}'$ isomerizes to $^3\mathbf{b}_1$ (HNCNOH) via 1, 2-H shift ($\mathbf{TS^3b'/^3b_1}$), followed by dissociation to produce either $\mathbf{P}_2$ (HNC + HNO) via a C–N1 bond rupture transition state $\mathbf{TS^3b_1/P_2}$ or $\mathbf{P}_8$ (O + HNCNH) via O elimination from $^3\mathbf{b}_1$ ($\mathbf{TS^3b_1/P_8}$). The barrier height of $\mathbf{TS^3b'/^3b_1}$, $\mathbf{TS^3b_1/P_2}$, and $\mathbf{TS^3b_1/P_8}$ are 12.9, −18.1, and −9.8 kcal/mol, respectively. The involved barrier height of $\mathbf{TS^3b'/^3b_1}$ (12.9 kcal/mol) makes the two pathways not competitive, either. These processes can simply be written as

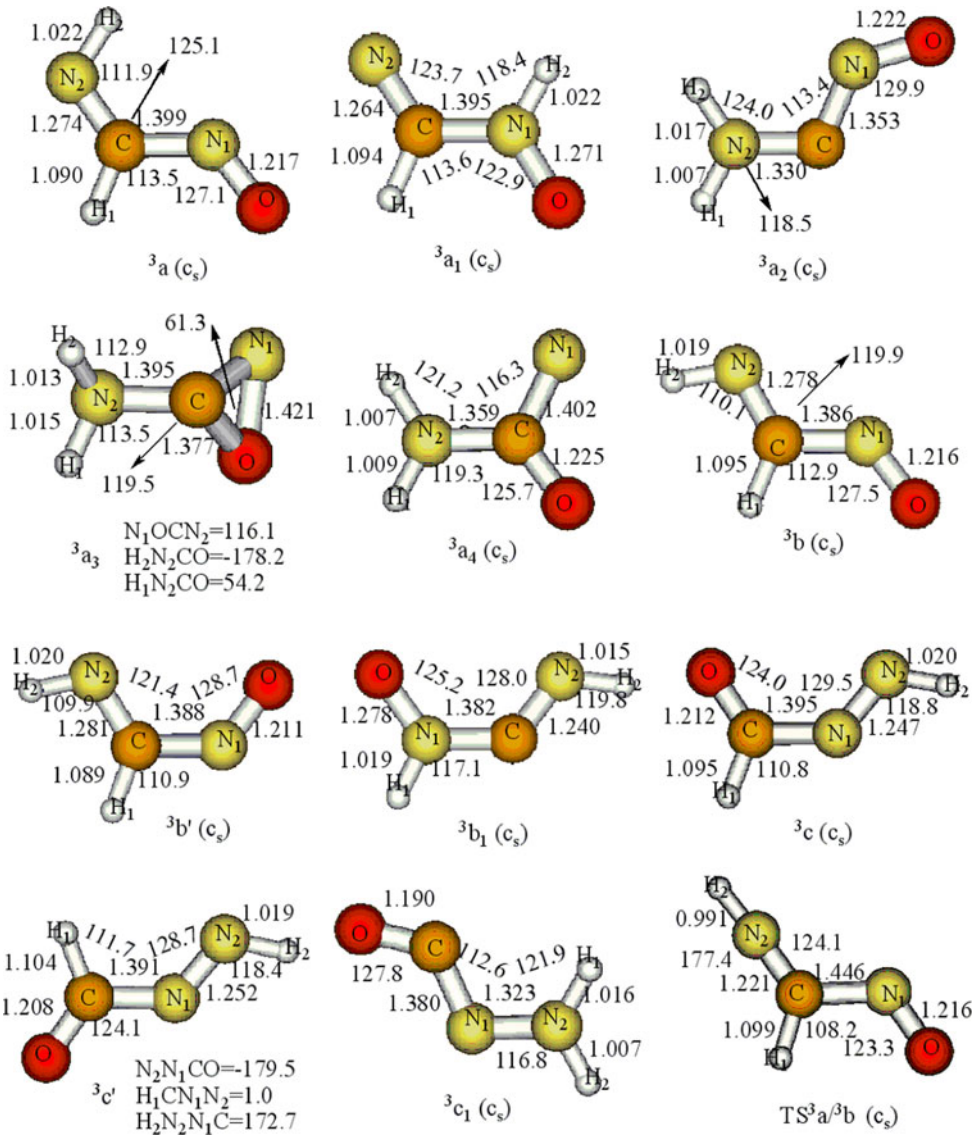

Fig. 3 UB3LYP/6-311 ++G(d, p) optimized geometries of isomers and transition states. Bond distances are in angstroms and angles are in degrees

Path 12 : $\mathbf{R} \rightarrow {}^3\mathbf{b} \rightarrow {}^3\mathbf{b}' \rightarrow {}^3\mathbf{b}_1 \rightarrow \mathbf{P_2}(\mathrm{HNC} + \mathrm{HNO})$

Path 13 : $\mathbf{R} \rightarrow {}^3\mathbf{b} \rightarrow {}^3\mathbf{b}' \rightarrow {}^3\mathbf{b}_1 \rightarrow \mathbf{P_8}\,(\mathrm{O} + \mathrm{HNCNH})$.

3.2.2 The nitrogen-to-nitrogen approach

The isomer ^{3}**c** (*cis*-OCHNNH) was formed via a non-planar three-membered transition state **TSR**/^{3}**c** (51.9 kcal/mol), the planar isomer ^{3}**c** can isomerize to planar isomer ^{3}**c**′ (*trans*-OCHNNH) via a C–N1 bond rotation process **TS**^{3}**c**/^{3}**c**′ with the barrier of 6.5 kcal/mol, then ^{3}**c**′ isomerizes to ^{3}**c**$_1$ (OCNNHH) via 1, 3-H shift (**TS**^{3}**c**′/^{3}**c**$_1$). Besides the decomposition of ^{3}**c**$_1$ to **P**$_3$ (NH_2 + NCO) via N1–N2 bond rupture transition state **TS**^{3}**c**$_1$/**P**$_3$ (−31.3 kcal/mol), ^{3}**c**$_1$ can decompose to **P**$_4$ (N_2H_2 + CO) via **TS**^{3}**c**$_1$/**P**$_4$ (−53.0 kcal/mol). For the barrier height of the initial transition state **TSR**/^{3}**c** 51.9 kcal/mol above the reactants, the two pathways are also not competitive. These processes can be described as

Path 14 : $\mathbf{R} \rightarrow {}^3\mathbf{c} \rightarrow {}^3\mathbf{c}' \rightarrow {}^3\mathbf{c}_1 \rightarrow \mathbf{P_3}(\mathrm{NH_2} + \mathrm{NCO})$

Path 15 : $\mathbf{R} \rightarrow {}^3\mathbf{c} \rightarrow {}^3\mathbf{c}' \rightarrow {}^3\mathbf{c}_1 \rightarrow \mathbf{P_4}(\mathrm{N_2H_2} + \mathrm{CO})$

In view of all these processes, the Path 10, starting from adduct ^{3}**a** leading to product **P**$_1$, should be the most competitive pathway for all isomers and transition states involved in this channel lying below the reactants. The other triplet pathways may contribute less to the NH ($X^3\Sigma^-$) + HCNO reaction compared with the singlet pathways.

Fig. 3 continued

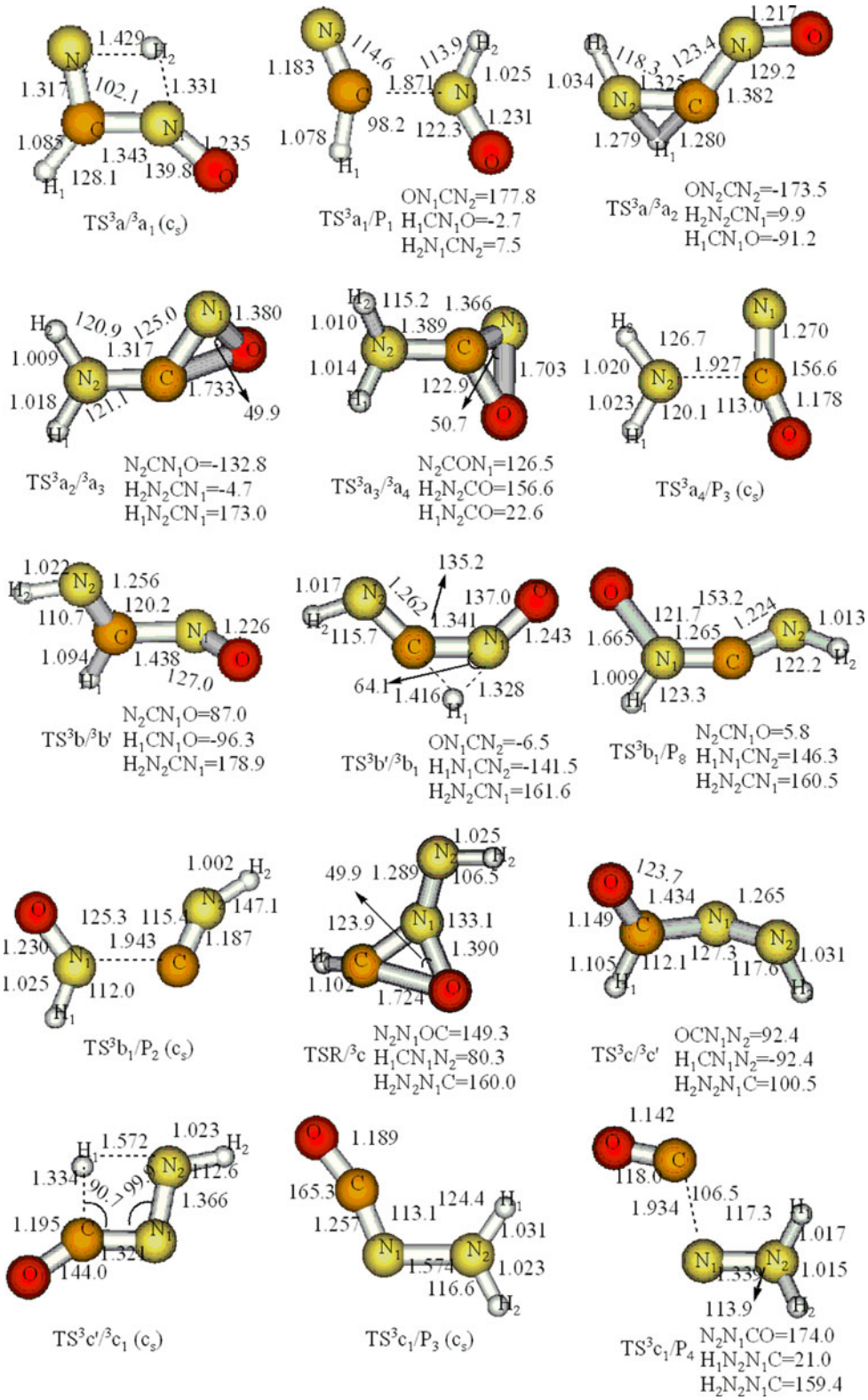

4 Conclusions

Both the singlet and triplet potential energy surfaces of the NH $(X^3\Sigma^-) + HCNO$ reaction system have been characterized in detail at the UB3LYP level for the geometry optimization, and at the UQCISD(T), UCCSD(T) and BMC-CCSD levels for the single-point energy. The mechanism can generally be summarized as association,

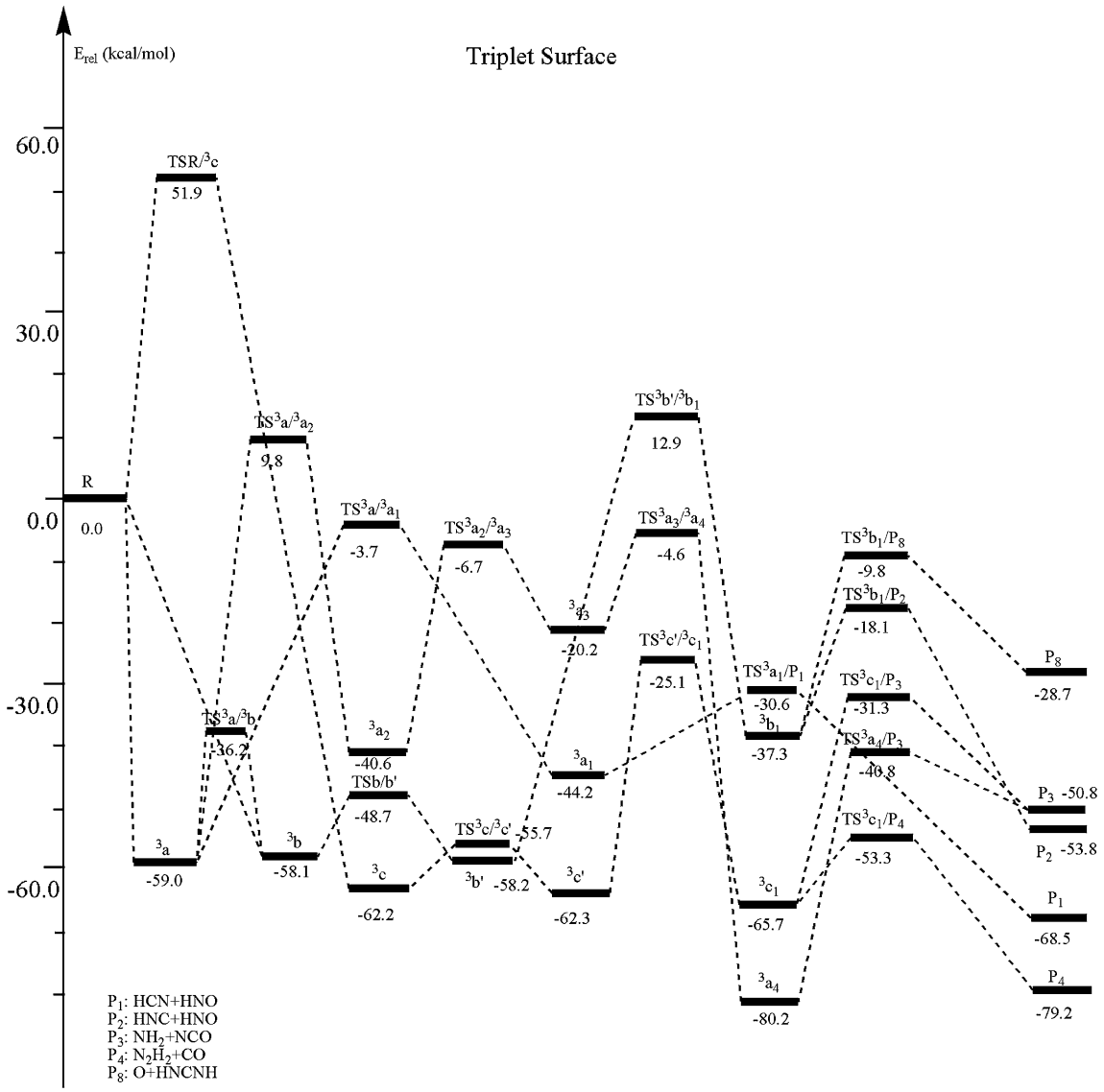

Fig. 4 Schematic potential energy surface of the reaction channels for the NH ($X^3\Sigma^-$) + HCNO reaction in triplet. Relative energies (E_{rel}, kcal/mol) are calculated at the BMC-CCSD//UB3LYP/6-311++G(d, p) level

isomerization and dissociation process. In singlet, (1) This reaction is most likely initiated by the nitrogen-to-carbon approach to form adducts **a** (*trans*-HNCHNO) and **b** (*cis*-HNCHNO) without barriers. Although nitrogen-to-nitrogen approach can lead to **c** (HC(O)NNH) which lies below the reactants **R** by 95.9 kcal/mol, the high-lying transition state **TSR/c** (0.7 kcal/mol) effectively blocks the formation of **c** at normal temperatures. (2) For the NH ($X^3\Sigma^-$) + HCNO reaction, four kinds of products $\mathbf{P_1}$ (HCN + HNO), $\mathbf{P_2}$ (HNC + HNO), $\mathbf{P_3}$ (NH_2 + NCO) and $\mathbf{P_4}$ (N_2H_2 + CO) should be observed. Among these products, $\mathbf{P_1}$ and $\mathbf{P_2}$ should be the major products. Especially, $\mathbf{P_1}$ is the most favorable product, whereas $\mathbf{P_2}$ is the less competitive product. $\mathbf{P_3}$ and $\mathbf{P_4}$ are the minor products. Formation of $\mathbf{P_5}$ (H_2 + N_2 + CO), $\mathbf{P_6}$ (CH_2O + N_2), and $\mathbf{P_7}$ (HCOH + N_2) may become kinetically feasible at high temperature. In triplet, the Path 10, starting from adduct ^{3}**a** (*trans*-HNCHNO) leading to product $\mathbf{P_1}$ via 1, 3-H shift and C–N1 bond cleavage, should be the most feasible pathway for all isomers and transition states involved in this channel lying below the reactants ***R***. In conclusion, the NH ($X^3\Sigma^-$) + HCNO reaction is expected to be fast in singlet, and have very less competitive abilities in triplet pathways.

The present theoretical studies can provide useful information for further experimental investigation on the title reaction and are expected to be helpful for understanding the combustion chemistry of nitrogen containing compounds.

Acknowledgments This work is supported by the Training Fund of NENU'S Scientific Innovation Project (NENU-STC07016).

References

1. Miller JA, Klippenstein SJ, Glarborg P (2003) Combust Flame 135:357
2. Feng W, Meyer JP, Hershberger JF (2006) J Phys Chem A 110:4458
3. Feng W, Hershberger JF (2007) J Phys Chem A 111:3831
4. Feng W, Hershberger JF (2007) J Phys Chem A 111:10654
5. Zhang W, Du B, Feng C (2007) Chem Phys Lett 442:1
6. Li BT, Zhang J, Wu HS, Sun GD (2007) J Phys Chem A 111:7211
7. Wang S, Yu JK, Ding DJ, Sun CC (2008) Chem J Chin Univ 29:365
8. Wang S, Yu JK, Ding DJ, Sun CC (2007) Chem J Chin Univ 28:1329
9. Feng W, Hershberger JF (2008) Chem Phys Lett 457:307
10. Miller JA, Bowman CT (1989) Prog Energy Combust Sci 15:287
11. Alexander MH, Dagdigian PJ, Jacox ME, Colb CE, Melius CF, Rabits H, Smoke MD, Tsang W (1991) Energy Combust Sci 17:263
12. Hack W (1998) NH radical reactions review artical. In: Alfassi ZB (ed) N-centered radicals. Wiley, Chichester, pp 413–466
13. Smoot LD, Hill SC, Xu H (1998) Prog Energy Combust Sci 24:385
14. Lyon RK (1987) En Viron Sci Technol 21:231
15. Li Y, Liu HL, Sun YB, Li Z, Huang XR, Sun CC (2009) Theor Chem Acc 124:123
16. Frisch MJ, Trucks GW, Schlegel HB et al (2004) Gaussian 03, revision C.02. Gaussian, Inc, Wallingford
17. Becke AD (1993) J Chem Phys 98:5648
18. Lee C, Yang W, Parr RG (1988) Phys Rev B 37:785
19. Gonzalez C, Schlegel HB (1989) J Chem Phys 90:2154
20. Gonzalez C, Schlegel HB (1990) J Phys Chem 94:5523
21. Pople JA, Head-Gordon M, Raghavachari K (1987) J Chem Phys 87:5968
22. Lynch BJ, Zhao Y, Truhlar DG (2005) J Phys Chem A 109:1643
23. Lide DR (2003) CRC handbook of chemistry and physics, 80th edn. CRC, Boca Raton
24. Kuchitsu K (1998) Structure of free polyatomic molecules: basic data. Springer, Berlin
25. Liu JJ, Feng JK, Ding YH, Ren AM, Wang SF, Sun CC, Kong FA (2001) J Phys Chem A 105:5885
26. Huber KP, Herzberg G (1979) Molecular spectra and molecular structure (IV). Constants of diatomic molecules. Van Nostrand Reinhold, New York
27. NIST Chemistry WebBook (2005) NIST standard reference database number 69 (vibrational frequency data compiled by Jacox ME)
28. Gazdy B, Musaev DG, Bowman JM, Morokuma K (1995) Chem Phys Lett 237:27
29. Bowman JM, Gazdy B, Bentley JA, Lee TJ, Dateo CE (1993) J Chem Phys 99:308
30. Wang S, Yu JK, Ding DJ, Sun CC (2007) Theor Chem Acc 118:337